h, resonances attributable to **4**[1a] were at a maximum. The sample was then warmed to room temperature; after 1 h, **3** (δ 0.60, s, 18 H) was present in 85% yield (relative to total phenyl protons). An aliquot was diluted with heptane for an IR spectrum: 2027 m, 2013 s cm^{-1}. A similar experiment was conducted to obtain a ^{13}C NMR spectrum (ppm, C_6D_6): 212.4, 7.2.

Reaction of 3 with Na/Hg. Petroleum ether (30 mL) containing **3** (68 mg, 0.14 mmol) was stirring for 0.5 h over an amalgam of Na (61 mg, 2.6 mmol) and Hg (3 mL). $(C_2H_5)_2O$ (20 mL) was added and the solution decanted and filtered. The amalgam residue was washed with additional $(C_2H_5)_2O$ and filtered. Solvent was removed from the combined filtrates to yield **2c** (48 mg, 64%) as a light pink powder.

Acknowledgment. We are grateful to the National Science Foundation for support of this research (Grant No. CHE79-10580) and providing (via departmental grants) the FT NMR spectrometers used in this study. We also thank Professor O. L. Chapman and his research group for the use of their Rayonet photochemical reactor.

Registry No. **1**, 53248-31-0; **2a**, 78240-74-1; **2b**, 78465-74-4; **2c**, 79483-28-6; **2d**, 79483-29-7; **3**, 79483-30-0; $K_2Fe(CO)_4$, 16182-63-1; $Na_2Fe(CO)_4$, 14878-31-0; $Fe(CO)_5$, 13463-40-6; $(CH_3)_3SiBr$, 2857-97-8; $(CH_3)_3SiH$, 993-07-7; CF_3SO_3H, 1493-13-6; $(CO)_4FeHSi(CH_3)_3$, 63022-27-5.

Contribution from the Department of Chemistry, Texas A&M University, College Station, Texas 77843

Electronic Structure of Metal Clusters. 1. Photoelectron Spectra and Molecular Orbital Calculations on (Alkylidyne)tricobalt Nonacarbonyl Clusters

PETER T. CHESKY and MICHAEL B. HALL*

Received April 21, 1981

Ultraviolet photoelectron (PE) spectra and molecular orbital (MO) calculations are reported for several (alkylidyne)tricobalt nonacarbonyl compounds, $RCCo_3(CO)_9$, where R = H, CH_3, OCH_3, Cl, Br, and I. The molecular ionization energies from the PE spectra are closely related to the valence-orbital electronic structure. The MO calculations are helpful in assigning the spectra, in confirming the interpretation of trends, and in providing a consistent description of the electronic structure. The lowest energy ionization corresponds to a delocalized orbital which is both Co–C and Co–Co bonding. This ionization is followed closely by bands due to the Co–Co bonds and Co–CO π bonds. Well separated from these ionizations are those which correspond to Co–C bonding orbitals. The origin of this molecular orbital pattern is described both as the joining of three $Co(CO)_3$ fragments with a RC fragment and as the perturbation of a CCo_3 cluster by nine CO ligands and one R ligand. Although both descriptions are equally valid, the former provides a simpler interpretation of the MO results and PE spectra. Comparison of the PE spectra of H_3CX, $HC{\equiv}CX$, C_6H_5X, and $(CO)_9Co_3CX$ for the halogens suggests that the π bonding of the cobalt cluster to the apical C is much closer to $HC{\equiv}CX$ or C_6H_5X than it is to H_3CX. Both the PE spectra and MO calculations suggest that the apical carbon is electron rich but that the π system is sufficiently flexible to act as either a donor or acceptor. A localized MO description with an sp-hybridized C, in which a lone pair forms a dative bond to the metal triangle and the remaining p orbitals form multicentered π bonds to the Co_3 system, is consistent with all experimental evidence. If these ideas are extended to other systems, the hybridization at any carbon atom is determined primarily by the geometry of its non-transition-metal substituents. Thus, the CR group is best described as sp hybridized regardless of whether it is bound to a single metal or bridging three metals.

Introduction

The (alkylidyne)tricobalt nonacarbonyls are the oldest examples of heteronuclear cobalt carbonyl clusters.[1] Of all organometallic clusters, these have the most thoroughly explored organic chemistry.[2] Several review articles[2a,3] which cover both chemical and structural properties have appeared. Apart from the interest in their organic chemistry, suggestions have been made that discrete metal clusters may serve as models for miniature metal surfaces or highly dispersed, supported catalysts.[4]

The first crystal structure,[5] which was of $CH_3CCo_3(CO)_9$, confirmed a geometry consisting of a triangle of cobalts each with three carbonyls, capped by the CH_3C group, **1**. Simple

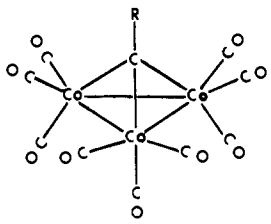

1

electron counting shows that the cluster is electron precise and the bonding can be described as 2-center, 2-electron bonds between atoms in the Co_3C core. Such a bonding picture is shown in **2**, where each line represents a 2-electron bond, and suggests an apical carbon with sp^3 hybridization.

(1) Markby, R.; Wender, I.; Fridel, R. A.; Cotton, F. A.; Sternberg, H. W. *J. Am. Chem. Soc.* **1958**, *80*, 6529.

(2) (a) Seyferth, D. *Adv. Organomet. Chem.* **1976**, *14*, 97. (b) Seyferth, D.; Eschback, C. S.; Nestle, M. O. *J. Organomet. Chem.* **1975**, *97*, C11. (c) Seyferth, D.; Williams, G. H.; Eschbach, C. S.; Nestle, M. O.; Merola, J. S.; Hallgren, J. E. *J. Am. Chem. Soc.* **1979**, *101*, 4867 and references within. (d) Seyferth, D.; Williams, G. H.; Traficante, D. D. *Ibid.* **1974**, *96*, 604. (e) Seyferth, D.; Williams, G. H.; Hallgren, J. E. *Ibid.* **1973**, *95*, 266. (f) Seyferth, D.; Williams, G. H.; Nivert, C. L. *Inorg. Chem.* **1977**, *16*, 758. (g) Seyferth, D.; Rudie, C. N. *J. Organomet. Chem.* **1980**, *184*, 365. (h) Seyferth, D.; Rudie, C. N.; Merola, J. S.; Berry, D. H. *Ibid.* **1980**, *187*, 91.

(3) (a) Palyi, G.; Placenti, F.; Markó, L. *Inorg. Chim. Acta, Rev.* **1970**, *4*, 109. (b) Penfold, B. R.; Robinson, B. H. *Acc. Chem. Res.* **1973**, *6*, 73. (c) Schmid, G. *Angew. Chem., Int. Ed. Engl.* **1978**, *17*, 392. (d) Schmid, G. *Angew. Chem.* **1978**, *90*, 417. (e) Dickson, R. S.; Fraser, P. J. *Adv. Organomet. Chem.* **1974**, *12*, 323.

(4) (a) Tolman, C. A. *Chem. Soc. Rev.* **1972**, *1*, 337. (b) Muetterties, E. L. *Bull. Soc. Chim. Belg.* **1975**, *84*, 959. (c) *Ibid.* **1976**, *85*, 451. (d) Ugo, R. *Catal. Rev.–Sci. Eng.* **1975**, *11*, 225. (e) Vahrenkamp, H. *Struct. Bonding (Berlin)* **1977**, *32*, 11.

(5) Sutton, P. W.; Dahl, L. F. *J. Am. Chem. Soc.* **1967**, *89*, 261.

0020-1669/81/1320-4419$01.25/0

Electrochemical studies[6] showed a facile, reversible one-electron reduction but decomposition upon oxidation or upon two-electron reduction. The ESR of the radical anions[7] has been interpreted as having an unpaired electron in a nondegenerate, metal–metal antibonding orbital of a_2 symmetry. A low-lying Co–Co antibonding orbital is also consistent with the photochemical cleavage of the Co–Co bond, which leads to the breakdown of the cluster.[8] The overall stability of the Co_3CR moiety is attested to by a strong peak in the mass spectra[9] due to the Co_3CR^+ ion. Further fragmentation suggests that the C–Co bonds are stronger than the Co–Co bonds. The Co_3C unit is also stable through a variety of chemical transformations and is the end product of numerous reactions with cobalt carbonyls.[2,3]

Most of the above results can be interpreted within the framework of the sp^3-localized bond model, **2**. However, hints

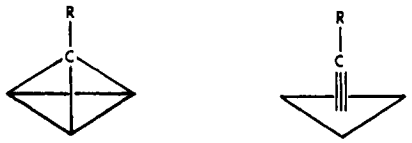

2 **3**

that the bonding was more delocalized than implied by resonance structure **2** came from early IR studies.[3a,10] On the basis of their ^{59}Co and ^{35}Cl NQR studies and previous work, Miller and Brill[11] suggested an sp-hybridized carbon and a carbyne-type resonance structure, **3**, in which the Co withdraws electron density from the apical substituent. The recent syntheses of numerous stable carbonium ions[2] containing this cluster suggest delocalized bonding with electron donation from the cluster to the apical carbon and its substituent. This apparent dichotomy was recognized much earlier and explained as the $(CO)_9Co_3C$ group possessing a flexible π system much like that of a phenyl ring.[3a]

An excellent qualitative discussion of the bonding in these and related clusters has been provided by the recent work of Schilling and Hoffmann.[12] Nevertheless, there remain questions of a more quantitative nature about the ordering of the one-electron orbitals, the overall charge distribution, and the best localized bond picture. For these reasons we have undertaken a study of these complexes using gas-phase, UV photoelectron (PE) spectroscopy and Fenske–Hall[13] molecular orbital (MO) calculations.[14]

Experimental and Theoretical Section

Preparation. All operations were performed in an inert atmosphere of dry nitrogen or argon. All nonchlorinated solvents were dried over sodium benzophenone and distilled under nitrogen immediately before use. Chlorinated solvents were dried with molecular sieves followed by calcium hydride. Dicobalt octacarbonyl was purchased from Pressures Chemical Co., Pittsburgh, PA. Other organic starting materials were purchased from Aldrich Chemical Co., Milwaukee, WI, and used without further purification. The (alkylidyne)tricobalt nonacarbonyls were prepared from standard published procedures[10,15] with the exception of the iodo complex.[16] All compounds were purified by vacuum sublimation and verified by both melting points and IR spectroscopy. The IR spectra were recorded on a Perkin-Elmer 297 IR spectrometer. The samples were prepared and run in Nujol mulls.

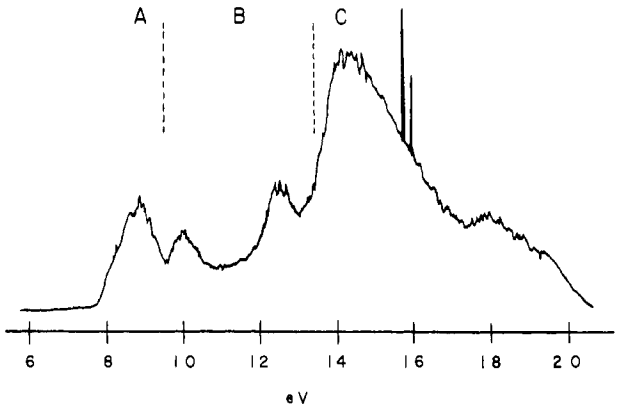

Figure 1. Photoelectron spectrum of (chloromethylidyne)nonacarbonyl-*triangulo*-tricobalt.

Spectroscopy. The ultraviolet photoelectron spectra were taken on a Perkin-Elmer Model PS-18 Spectrometer. The total spectrum was recorded as a single slow scan, and the argon $^2P_{3/2}$ and $^2P_{1/2}$ lines at 15.75 and 15.94 eV were used as the internal reference. The resolution for all spectra was better than 37 meV for the fwhm of the Ar $^2P_{3/2}$ peak.

Theoretical Procedures. Fenske–Hall MO calculations[13] (nonempirical, self-consistent-field) were performed on an Amdahl 470 V/6 computer. The cobalt basis functions (1s through 3d) were taken from Richardson et al.[17] and were augmented by a 4s and 4p function with an exponent of 2.0. The carbon, oxygen, and halogen functions were taken from the double-ζ functions of Clementi[18] and reduced to a single-ζ function,[19] except for the p valence functions which were retained as the double-ζ function. An exponent of 1.2 was used for the hydrogen atom. The atomic functions were made orthogonal by the Schmidt procedure. Mulliken population analysis was used to determine both the individual atomic charges and atomic orbital populations.

The atomic positions for the (alkylidyne)tricobalt nonacarbonyl clusters were idealized to C_{3v} symmetry from published structural studies.[5] Bond lengths between the apical carbon atom and the R group were estimated as standard bond lengths.

Results

Photoelectron Spectra. The complete spectrum of (chloromethylidyne)nonacarbonyl-*triangulo*-tricobalt is shown in Figure 1. The spectrum is divided into three regions: A (6.0–9.5 eV), B (9.5–13.5 eV), and C (13.5–20.0 eV). In region A the spectrum shows one broad band with a maximum at 8.8 eV. The band displays a distinct shoulder on the low-energy side and is fairly broad near the maximum which indicates several closely spaced ionizations. There are two bands in region B: one at 10.0 and another at 12.4 eV. A very broad intense band begins in region C and reaches maximum intensity at 14.1 eV. The two spikes on the high-energy side of this band corresponds to the $^2P_{3/2}$ and $^2P_{1/2}$ Ar lines, respectively. At about 18.0 eV, a weaker broad band is also apparent. Since region C is similar in the spectra for

(6) (a) Kotz, J. C.; Peterson, J. V.; Reed, R. C. *J. Organomet. Chem.* **1976**, *120*, 433. (b) Bond, A. M.; Peake, B. M.; Robinson, B. H.; Simpson, J.; Watson, D. J. *Inorg. Chem.* **1977**, *16*, 410.
(7) (a) Matheson, T. W.; Peake, B. M.; Robinson, B. H.; Simpson, J.; Watson, D. J. *J. Chem. Soc., Chem. Commun.* **1973**, 894. (b) Peake, B. M.; Robinson, B. H.; Simpson, J.; Watson, D. J. *Inorg. Chem.* **1977**, *16*, 405.
(8) Geoffroy, G. L.; Epstein, R. A. *Inorg. Chem.* **1977**, *16*, 2795.
(9) (a) Mayes, M. J.; Simpson, R. M. F. *J. Chem. Soc. A* **1968**, 1444. (b) Robinson, B. H.; Than, W. S. *Ibid.* **1968**, 1784.
(10) (a) Dent, W. T.; Duncanson, L. A.; Guy, R. G.; Reed, H. W. B.; Shaw, B. L. *Proc. R. Soc. London, Ser. A* **1961**, 169. (b) Bor, G.; Markó, B.; Markó, L. *Chem. Ber.* **1962**, *95*, 333.
(11) Miller, D. C.; Brill, T. B. *Inorg. Chem.* **1978**, *17*, 240.
(12) Schilling, B. E.; Hoffmann, R. *J. Am. Chem. Soc.* **1978**, *100*, 6274; **1979**, *101*, 3456.
(13) Hall, M. B.; Fenske, R. F. *Inorg. Chem.* **1972**, *11*, 768.
(14) Presented in part at the 35th Southwest Regional Meeting of the American Chemical Society, Austin, TX, Dec 5–7, 1979; Abstract 137.
(15) (a) Seyferth, D.; Hallgren, J. E.; Hung, P. L. K. *J. Organomet. Chem.* **1973**, *50*, 265. (b) Seyferth, D.; Nestle, M. O.; Hallgren, J. E.; Merola, J. S.; Williams, G. H.; Nivert, C. L. *Inorg. Synth.* **1980**, *20*, 224.
(16) Ercoli, R.; Santambrogio, E.; Casagrande, G. T. *Chim. Ind. (Milan)* **1962**, *44*, 1344.
(17) Richardson, J. W.; Nieuwpoort, W. C.; Powell, R. R.; Edgell, W. F. *J. Chem. Phys.* **1962**, *36*, 1057.
(18) Clementi, E. *J. Chem. Phys.* **1964**, *40*, 1944; *IBM J. Res. Dev.* **1965**, *9*, 2.
(19) Fenske, R. F.; Radtke, D. D. *Inorg. Chem.* **1968**, *7*, 479.

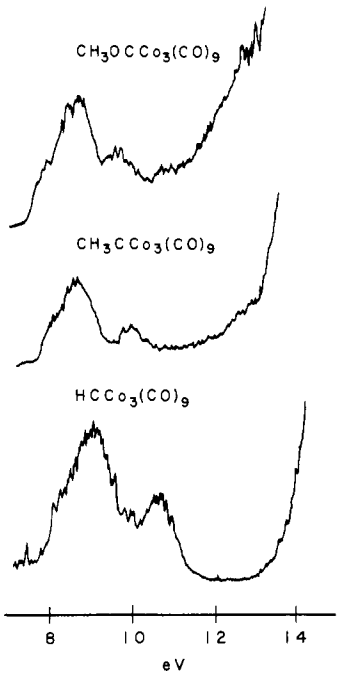

Figure 2. Partial photoelectron spectra for the hydrido, methyl, and methoxy compounds.

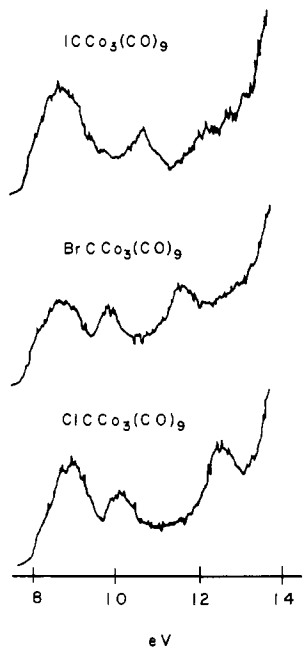

Figure 3. Partial photoelectron spectra for the chloro, bromo, and iodo compounds.

all the compounds, only the lower energy regions (A and B) will be shown for the remaining spectra.

Regions A and B for the hydrido, methyl, and methoxy compounds are shown in Figure 2. The band in region A displays a maximum at 8.8, 8.7, and 8.6 eV for the hydrido, methyl, and methoxy, respectively. The low-energy shoulder is very apparent in these spectra. The second peak in the spectra (first in region B) occurs at 10.4, 9.9, and 9.6 eV, respectively. For the hydrido compound there are no other ionizations before the onset of the characteristic band of region C at about 14 eV. The methyl compound has a very weak band at 13 eV, while the methoxy compound has a more intense feature which begins at 12 eV and has a maximum at 12.7 eV.

The low-energy regions of the halogen spectra are shown in Figure 3. The spectrum of the bromo compound is similar to that of the chloro. The first band (region A) has its maximum at 8.9 eV. Region B contains two bands, one at 9.8 and another at 11.6 eV. The iodo spectrum shows a more intense first band with a maximum at 8.7 eV and a weak feature on the high-energy side at about 9.7 eV. Region B has one distinct band at 10.6 eV and a weak feature beginning at 12.3 eV.

Molecular Orbital Calculations. Although MO calculations were made on all of the compounds, only the electronic structure of the (chloromethylidyne)nonacarbonyl-*triangulo*-tricobalt will be presented in detail. The other compounds in this series are closely related, and only the more important, less obvious differences will be mentioned explicitly. In large molecules the complexity of the MO pattern, caused by a large number of closely spaced MO's, becomes difficult to interpret. To simplify this problem one can analyze the MO's of the molecule in terms of smaller component parts. One approach is fragment analysis where one views $RCCo_3(CO)_9$ as formed from three $Co(CO)_3$ groups and one CR group. This approach was used by Schilling and Hoffmann in their description of M_3L_9 complexes.[12] A second approach, which we will call cluster analysis, begins with the tetranuclear cluster CCo_3 and considers how nine CO's and one R group perturb the CCo_3 cluster in forming the compound. We will describe both approaches in the next two sections. The numbering of the molecular orbitals of the clusters and fragments begins with the lowest energy valence molecular orbitals, except for CO where the 1σ and 2σ are the O 1s and C 1s, respectively.

Fragment Analysis. The lowest lying molecular orbitals of the $Co(CO)_3$ fragment, which was idealized to C_{3v} symmetry, consist of symmetry adapted combinations of the carbonyl's 3σ, 4σ, and 1π. The next group of orbitals ($4a_1$, 5e), which form the Co–CO σ bonds, involve donation from the carbonyl's 5σ orbitals to the metal orbitals. At much higher orbital energy are the 6e and $5a_1$ molecular orbitals, which are primarily Co 3d in character (83%). These orbitals, which are stabilized by interaction with the 2π orbitals of the carbonyls, correspond to the t_{2g} orbitals of an octahedral (O_h) system such as $Cr(CO)_6$. The 7e pair, which is destabilized by interaction with the 5σ CO, corresponds to the e_g orbitals of an O_h system, but it contains about 15% 4p in addition to the 3d. In the neutral $Co(CO)_3$ fragment, the 7e orbitals are the highest occupied molecular orbitals (HOMO) with 3 electrons. The lowest unoccupied molecular orbital (LUMO) is the $6a_1$, which is a mixture of 4s, 4p, and 2π CO. The most important orbitals for the formation of the cluster (6e, $5a_1$, 7e, and $6a_1$) are shown with their major parentage on the left of Figure 4.

The most important molecular orbitals of the CCl diatomic unit are also shown in Figure 4. The 1π MO corresponds to a C–Cl π bond strongly polarized toward Cl (82% Cl). The 3σ corresponds to a C lone pair, similar to the 5σ of CO. The HOMO of this moiety, the 2π, contains 1 electron and is C–Cl π antibonding with primarily C character (82%). At lower orbital energy and not shown in Figure 4 are the 1σ (3s Cl) and the 2σ (C–Cl σ bond).

In describing the formation of the final cluster $ClCCo_3(CO)_9$ from the fragments $Co(CO)_3$ and CCl, we will concentrate on the higher energy fragment orbitals shown in the second column of Figure 4. Although the lower energy fragment orbitals may be delocalized over the entire cluster, they do not contribute to cluster bonding. The 3σ of the CCl fragment interacts with the 7e and $6a_1$ to form the $12a_1$ (at 16 eV, not shown on Figure 4) which is completely cluster bonding. This MO may be thought of as a "lone pair" on the C of CCl that donates electron density to acceptor orbitals on the $Co_3(CO)_9$ cluster that are formed from the 7e and $6a_1$. The 1π orbital of CCl interacts with the 6e of the $Co(CO)_3$ fragments to form the 16e orbitals which are primarily Cl in character. The next

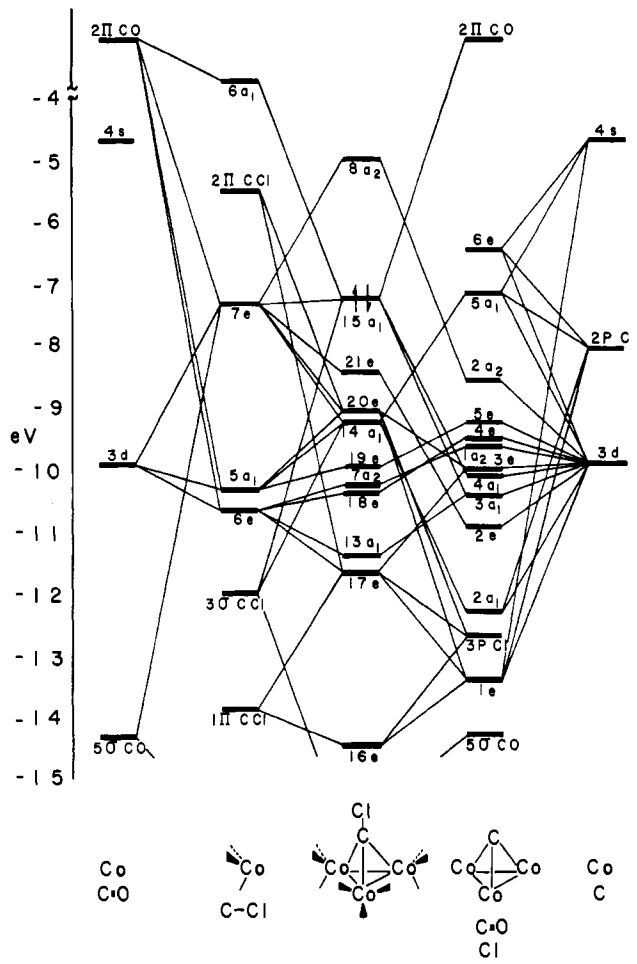

Figure 4. Molecular orbital bonding scheme for (chloromethylidyne)nonacarbonyl-*triangulo*-tricobalt. The energy values were obtained from a Fenske–Hall calculation. Connectivity lines indicate the principal contributions to each molecular orbital.

group of MO's, 17e, $13a_1$, 18e, and $7a_2$, are formed from the interaction of the 6e orbitals of the $Co(CO)_3$ fragments. The 17e also has contributions from both the 1π CCl and the 2π CCl and is destabilized by the former but stabilized by the latter. The $5a_1$ orbitals of the $Co(CO)_3$ moiety combine to form the 19e and $14a_1$. The $14a_1$ also contains significant contributions from the $Co(CO)_3$ 7e and CCl 3σ. The $Co(CO)_3$ 7e orbitals interact to form the 20e, 21e, $15a_1$, and $8a_2$ MO's. The 20e is stabilized by interaction with the 2π CCl orbital. The $15a_1$ is stabilized by interaction with the $6a_1$ $Co(CO)_3$ orbitals and destabilized by interaction with the 3σ CCl orbitals. The $15a_1$ and $8a_2$ are the HOMO and LUMO, respectively, of the full cluster, $ClCCo_3(CO)_9$.

In terms of the fragment analysis, it is clear that most of net cluster bonding involves the $Co(CO)_3$ fragment's 7e and $6a_1$ and the CCl fragment's 3σ and 2π. Thus, in the free neutral fragments the orbital populations are $7e^3$ $6a_1^0$ and $3\sigma^2$ $2\pi^1$, while in the final cluster molecule the populations are $7e^{2.5}$ $6a_1^{0.5}$ $3\sigma^{1.4}$ $2\pi^{1.9}$. The redistribution of these 12 electrons, donation from the 3σ to the 7e and $6a_1$, and donation from the 7e to the 2π constitute the primary bonding of the cluster. In the next section we will describe an alternative view of the origin of the final MO structure, and we will reserve a detailed discussion of the individual MO's until we have examined the orbital plots.

Cluster Analysis. We begin this analysis by assembling the tetranuclear cluster CCo_3 from one C atom and three Co atoms; the resulting MO diagram is shown on the right side of Figure 4. The lowest energy MO in CCo_3, the $1a_1$, corresponds closely to the C 2s and is not shown in Figure 4. The next 18 MO's, which are shown on Figure 4, are all those that can be formed from one C 2p and three Co 3d functions. The Co 4s also makes important contributions to some of these MO's (vide infra). Of these 18 MO's, the three lowest energy MO's (1e and $2a_1$) are greater than 50% C 2p in character. These orbitals also contain some in-plane Co–Co bonding interactions, especially the $2a_1$. The remainder of the Co–Co σ bonding (in-plane) resides primarily in the 2e and $3a_1$; the $3a_1$ also contains some Co–Co π bonding (out-of-plane). The $4a_1$ and 3e are weakly Co–Co bonding, while the $1a_2$, 4e, and 5e are weakly Co–Co antibonding. The remaining MO's contain substantial antibonding character. The $2a_2$ is in-plane Co–Co σ antibonding, while the $5a_1$ is nearly Co–Co nonbonding but Co–C antibonding with substantial 4s character. In a similar fashion the 6e is Co–C antibonding.

Since the primary C–Co bonds are the lowest energy MO's and contain more C than Co character, the CCo_3 cluster can be described formally as a carbide with substantial donation from the C^{4-} to the cobalts. The overall charge distribution on the neutral CCo_3 cluster is $C^{0.9-}$ and $Co^{0.3+}$. For the subsequent description of the entire molecule, it will be convenient to view the cluster as CCo_3^+, where the 5e is the HOMO with 4 electrons and the $2a_2$ is the LUMO.

When CCo_3^+, Cl^-, and nine CO's are brought together to form the final molecule, there is considerable rearrangement of the CCo_3^+ cluster MO's. The $3p_z$ orbital of Cl^- interacts with the $1a_1$ and $2a_1$ of the CCo_3^+ cluster forming the $9a_1$ and $12a_1$ MO's of the molecule (not shown in Figure 4) and pushing some $2a_1$ CCo_3^+ character into the $14a_1$. The $3p_\pi$ orbitals of Cl^- interact mainly with the 1e to form the 16e and 17e MO, but they contribute some Cl character to the 20e. The 5σ orbitals of the carbonyls, which are lower in energy than most of the CCo_3^+ cluster orbitals, donate electron density strongly to the $2a_2$, $5a_1$, 6e, 7e, $6a_1$, and 8e. These MO's, which were empty in the bare CCo_3^+ cluster, now have occupation numbers between 0.9 and 0.4 electrons. The 5σ interactions cause the M–CO σ bonding orbitals to be stabilized (not shown in Figure 4) and the previously empty cluster orbitals to be raised in energy (only the $8a_2$ is shown in Figure 4). Interaction with the 5σ CO's also destabilizes the $2a_1$, 2e, $3a_1$, $4a_1$, and 3e cluster orbitals in forming the $14a_1$, 20e, 21e, and $15a_1$. The $15a_1$ MO also has contributions from the 2π CO orbitals of greater than 30%. The 2π CO also contributes to the 21e, 20e, and $14a_1$ MO's. The primary 2π CO interactions are with the 5e, 4e, $1a_2$, 3e, and $3a_1$ cluster orbitals which are stabilized into the 19e, $7a_2$, 18e, $13a_1$, and 17e molecular orbitals. In forming the molecule the CCo_3^+ cluster donates 0.6 electron from each of the $2a_1$, $3a_1$, $4a_1$, 3e, $1a_2$, 4e, and 5e.

The two analyses presented above, fragment and cluster, are complementary and equally valid; however, the fragment analysis is conceptually simpler, at least in this system. This difference arises because the formation of the Co–CO bonds is a larger perturbation than the formation of the Co–Co bonds.

Molecular Orbital Plots. In cluster systems such as $ClCCo_3(CO)_9$, orbital maps are very helpful in elucidating the cluster bonding since individual bonds are often delocalized over several MO's. If one takes three equivalent Co–Co (or three equivalent C–Co) localized bond orbitals, their symmetry adapted combinations will form three MO's of a_1 and e symmetry. In the following discussion we will describe the main Co–Co and C–Co bonding orbitals in terms of these symmetry MO's.

Figure 5 shows contour plots of the MO's which are involved in Co–Co in-plane bonding. From the cluster point of view, the $12a_1$, $13a_1$, $14a_1$, and $15a_1$ are all Co–Co bonding. However, the net contributions of the first two MO's are partly

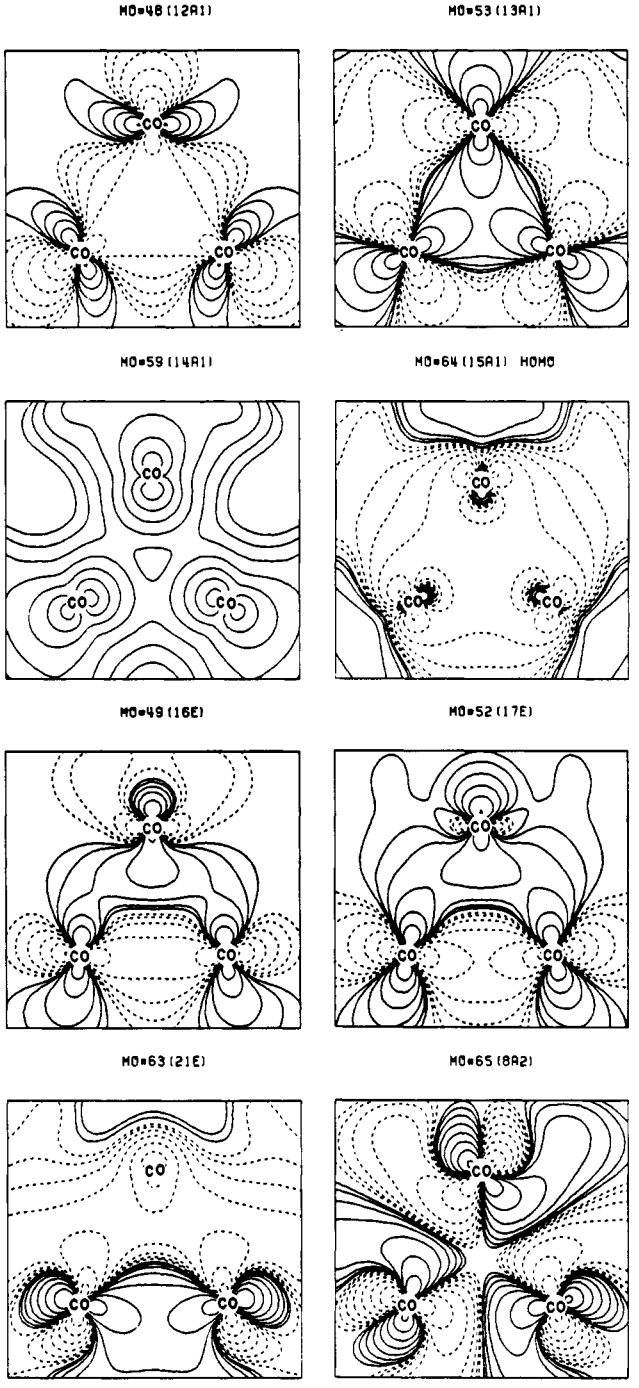

Figure 5. Orbital plots of the $12a_1$, $13a_1$, $14a_1$, $15a_1$, 16e, 17e, 21e, and $8a_2$ in the cobalt basal plane. The lowest contour values are $\pm 2.44 \times 10^{-4}$ e au^{-3}, and each succeeding contour differs from the previous one by a factor of 2.0.

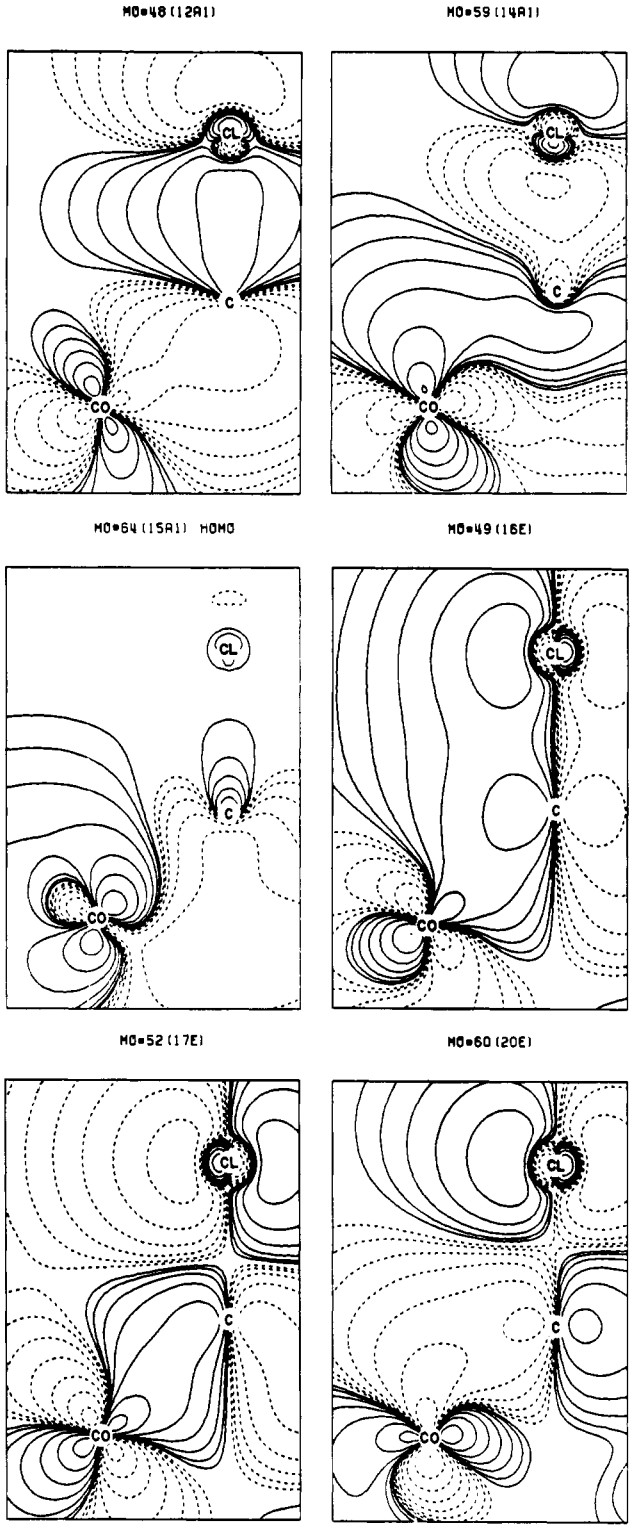

Figure 6. Orbital plots of the $12a_1$, $14a_1$, $15a_1$, 16e, 17e, and 20e in one of the chlorine–carbon–cobalt planes. The lowest contour values are $\pm 2.44 \times 10^{-4}$ e au^{-3}, and each succeeding contour differs from the previous one by a factor of 2.0.

cancelled by occupied antibonding orbitals and the net bonding arises primarily from the $14a_1$ and $15a_1$. Among the e symmetry orbitals, the 16e, 17e, and 21e (Figure 5) are all Co–Co bonding. Again the 16e and 17e are partly cancelled by occupied antibonding orbitals and the net bonding arises mainly in the 21e. From the fragment point of view, the Co–Co bonds originate from interaction of the $Co(CO)_3$ fragment's 7e and $6a_1$. These interactions are responsible for the formation of the $14a_1$, $15a_1$, and 21e, which we have identified as the primary Co–Co bonding orbitals. The HOMO, $15a_1$, is also delocalized over the carbonyls, while the LUMO, $8a_2$, is strongly localized on the metal and is Co–Co antibonding.

Figure 6 shows the most important C–Co bonding orbitals in one of the Cl–C–Co planes. From the cluster viewpoint the major fractions of the C–Co_3 "σ" bond is contained in the $12a_1$ and $14a_1$, both of which are also C–Cl bonding. The fragment analysis suggests that the $15a_1$ also contributes to the C–Co bond. The "π" bond between C and the Co_3 group is distributed primarily between the 16e, 17e, and 20e orbitals. The 16e is both C–Co and Cl–C bonding and is delocalized over all three atoms. The 17e is also C–Co bonding but is Cl–C antibonding. All three orbitals are important for the C–Co bond, but the fragment analysis emphasizes the 20e, which

is a more equal mixture of C and Co and contains less Cl character than either the 16e or 17e. The C–Co interactions are sufficiently strong that no C–Co antibonding orbitals are occupied to a significant degree.

Discussion

Photoelectron Spectra. Although care must be exercised in correlating calculated one-electron orbital energies with the ionization energies (IE's) observed in the PE spectra, previous experience with the Fenske–Hall approach has shown that reasonably good correlation can be obtained.[13,20] For the H, CH_3, and OCH_3 derivatives, the first band contains a large number of individual ionizations. At low energy there is a weak shoulder corresponding to ionization of electrons from the HOMO ($15a_1$), which is highly delocalized but is both Co–Co and Co–C bonding. This is followed by a more intense group of closely spaced ionizations which correspond to the main Co–Co bonding orbitals (21e), to part of the Co–C π system (20e), and to the Co–CO π bonding orbitals ("t_{2g}" in the $Co(CO)_3$ fragment).

The second band in the spectra is due to the Co–C "π" bond (17e) which is displayed qualitatively in **4**. This band shifts

4

strongly on substitution of a CH_3 group for H at the apical carbon. One also observes a smaller shift in the lowest IE which makes the shoulder on the first bond more prominent in the CH_3 derivative. Similar results have been observed in the PE spectra of $R_2C_2Co_2(CO)_6$.[21] The shift in the second band (17e) is a direct effect of the π-donor capacity of the methyl group, while the change in the leading edge is an indirect effect of the methyl group's ability to increase the electron density on the cluster. On substituting the OCH_3 group at the apical carbon, one sees a shift of the second band to lower IE but little change in the leading edge of the first band. These results are consistent with the HOMO being of a_1 symmetry and only indirectly affected by the increased π-donor ability of the apical substituent, and with the second band being Co–C π bonding (**4**) and strongly affected by the substitution at the apical carbon.

The band which begins at 14 eV in the spectrum of $HCCo_3(CO)_9$ is due to ionizations of the CO 5σ orbitals, which are involved in the Co–Co σ bonds, and of the CO 1π orbitals. In the methyl derivative there is a weak band preceding the characteristic CO ionizations which is due to the C–H bonding combination of e symmetry (**5**). It is the interaction of orbital

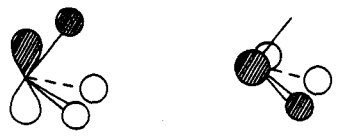

5

5 with orbital **4** which causes the strong shift in the position of the second band. In the methoxy derivative there is an additional contribution from an O "lone pair" in the region just before the onset of the C–H "e" band. Also, in this same region we would expect ionization from the C → Co_3 σ bond ($12a_1$), and this ionization may be responsible for some of the intensity around 13.5 eV in several of the spectra.

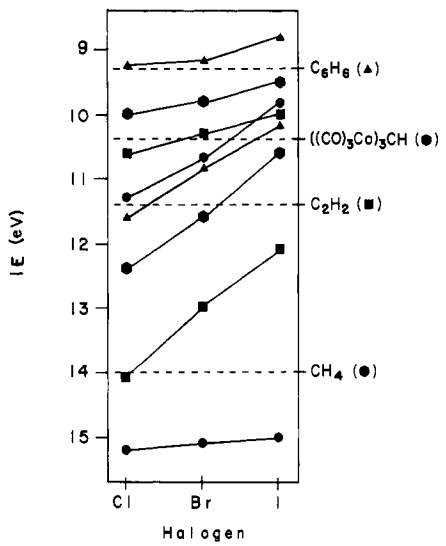

Figure 7. Correlation diagram showing the ionization energy of the symmetric and antisymmetric combination of the halogen π lone pair with the corresponding π orbital in the remaining fragments: C_6H_5X (triangle), $(CO)_9Co_3CX$ (hexagon), HC≡CX (square), and H_3CX (circle).

The order of the MO's and IE's presented above differs from that suggested by Schilling and Hoffmann.[12] In the most important difference, our results suggest that the apical substituent does become involved with the "t_{2g}" orbitals on the $Co(CO)_3$ fragments. This occurs most dramatically in the formation of the 17e, which appears as a well-separated ionization. Our theoretical results also suggest that the Co–Co bonding orbital, 21e, is at lower IE than the C–Co orbital, 20e, in contrast to the extended-Hückel results. Our interpretation of the spectra also differs from a recent report of the PE spectra of the fluoro, methyl, and chloro derivatives.[22]

The first and second bands in the spectra of the Cl and Br derivatives are similar to that of the H derivative, but both spectra display an additional band at 12.4 and 11.6 eV, respectively, which is due to the halogen lone pairs of π symmetry. The spectrum of the I derivative, at first, appears somewhat anomalous because it is missing a band. We believe that this is due to the increased π-donor ability of the I which interacts strongly with orbital **4** and causes it to merge into the first band. This accounts for the increased relative intensity of the first band in the I spectrum and the apparent loss of spin–orbit splitting usually seen in iodo derivatives. The weak feature at 12.3 eV is then due to the I–C σ bond and perhaps the C → Co_3 σ bond. Of all the compounds in this study, the I derivative proved to be the most difficult spectrum to obtain because of some degree of decomposition in the spectrometer. In spite of this problem, we believe the spectrum shown in Figure 3 is essentially correct. The first band in all three halogen derivatives (Cl, Br, I) shows a steady decrease in IE, reflecting the halogen's decreasing electronegativity.

Some insight into the bonding can be obtained by comparison of the IE for H_3CX,[23] HC≡CX,[24] C_6H_5X,[25] and

(20) (a) Lichtenberger, D. L.; Fenske, R. F. *Inorg. Chem.* **1976**, *15*, 2015. (b) Lichtenberger, D. L.; Fenske, R. F. *J. Am. Chem. Soc.* **1976**, *98*, 50. (c) Block, T. F.; Fenske, R. F. *Ibid.* **1977**, *99*, 4321. (d) Hubbard, J. L.; Lichtenberger, D. L. *Inorg. Chem.* **1980**, *19*, 1388. (e) Morris-Sherwood, B. J.; Kolthammer, B. W. S.; Hall, M. B. *Ibid.* **1981**, *20*, 2771.

(21) DeKock, R. L.; Lubben, T.; Hwang, J.; Fehlner, T. P. *Inorg. Chem.* **1981**, *20*, 1627.

(22) Granozzi, G.; Agnolin, S.; Casarin, M.; Osella, D. *J. Organomet. Chem.* **1981**, *208*, C6.

(23) Turner, D. W.; Baker, C.; Baker, A. D.; Brundle, C. R. "Molecular Photoelectron Spectroscopy"; Wiley: New York, 1970; Chapter 2.

(24) Haink, H. J.; Heilbronner, E.; Hornung, V.; Kloster-Jensen, E. *Helv. Chim. Acta* **1970**, *53*, 1073.

$((CO)_3Co)_3CX$. In Figure 7 we have drawn a correlation diagram showing the average IE of the symmetric and antisymmetric combination of the halogen π lone pair with the appropriate π orbital in the remaining fragment (**5** in H_3C, π bond in HC≡C and C_6H_6, and **4** in $((CO)_3Co)_3C$). The horizontal lines correspond to the IE of the H substituted derivative which has a π orbital on the fragment only. One can see immediately from the position of these IE's that the electronic structure at the apical C in the cobalt cluster is not intermediate between that of a simple sp^3 fragment (H_3C) and a simple sp fragment (HC≡C). The substantial difference between the cobalt cluster and "similar" organic compounds has lead to some confusion because of attempts to describe it as being analogous to one or the other. When H is substituted by a halogen there are now two π type IE's: one a lower IE and one at a higher IE than for the H derivative. In H_3CX the halogen π lone pairs are at low IE and are well separated from the π-type C–H orbitals, **5**. In HC≡CX the π acetylene orbitals are at lower IE's and mix more strongly with the halogens forming symmetric and antisymmetric combinations that have IE's higher and lower, respectively, than that for HC≡CH. Analysis of the spin–orbit coupling in HC≡CBr suggests that these combinations are nearly equal mixture for this molecule. This means that the lower IE band in HC≡CCl has more C π character than Cl π character, while in HC≡CI the lower IE has more I character. The π band in C_6H_6 is at an even lower IE than that of HC≡CH. The C_6H_5X derivative's IE pattern parallels those of HC≡CX, but mixing between phenyl π and halogen π does not become substantial until X = I. The $(CO)_9Co_3C$ fragment is even a better π donor than HC≡C and is just as strongly delocalized but with equal mixing of cluster π and halogen π occurring between Br and I. In some ways the $(CO)_9Co_3C$ group is intermediate between HC≡C and C_6H_5 in its π-bonding characteristics.

The interpretation of the PE spectra presented above strongly suggests that the apical carbon in the cobalt cluster is electron rich. This accounts for its ability to stabilize a variety of carbonium ions.[2] There is strong delocalization of the halogen π electrons and the $(CO)_9Co_3C$ π system as suggested by recent NQR experiments,[11] but the overall effect of the cobalt cluster is not electron withdrawing.

Nature of the Bonding. Although the complete MO model provides perhaps the best description of the electronic structure, a localized bond model which is consistent with the complete MO calculation and the PE spectra would be useful. None of the proposed resonance structures are completely satisfactory in this respect. The Co–Co bonds can be described as localized 2-center, 2-electron bonds. To describe the bonding of the RC group to the $Co_3(CO)_9$ fragment, we begin with an sp-hybridized C. One hybrid is used to bond to the R group, the other hybrid contains an electron pair which forms a dative bond by donating some of its electron density to the Co_3 triangle **6** or **7**. This bond corresponds closely to

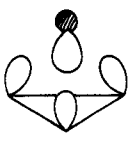

6

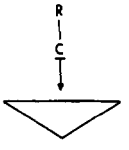

7

the $12a_1$ MO and is often too stable to be seen in the PE spectra before the onset of the characteristic CO region. The remaining 2p π orbitals on C combine with orbitals of the appropriate symmetry on the Co_3 triangle to form two multicenter, 2-electron bonds, **5** or **8**, much as in borane clusters.

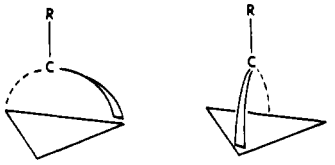

8

The 17e MO, whose ionization occurs near 10 eV, corresponds closely to these localized bonds. There would also be some admixture of the 20e in the fully localized Co–C π bonds.

If we may make a generalization based on our limited results, we would suggest that the hybridization at an organometallic carbon atom is based on the geometry of the organic fragment itself and not on the number of transition metals to which it is bound. Thus, C in the CR group is sp hybridized whether it is bound to one or several metals. For R′–C–R angles near 120°, the carbon in the carbene CRR′ is sp^2 hybridized both when terminal and when bridging two transition metals. How accurate these generalizations are remains to be seen. The accuracy depends on the metal orbitals being sufficiently higher in energy (lower IE) and sufficiently compact such that they are incapable of rehybridizing a carbon atom attached to them. Thus, the generalizations should hold best for first-row transition metals in low-oxidation states. In the series $[(RC)_n(Co(CO)_3)_{4-n}]$, the hybridization would evolve from near sp^3 in $(RC)_4$, tetrahedrane, to sp in $RC(Co(CO)_3)_3$. The hybridization at each stage would be determined primarily by the number and geometry of the nonmetal bonds.

In all of our calculations the lowest unoccupied orbital (LUMO) is of a_2 symmetry and is Co–Co antibonding. Although the PE spectra give us no clue as to the nature of this orbital, the ease of reduction of these clusters,[6] their ESR spectra,[7] and the photoinduced Co–Co bond cleavage[8] have all been interpreted as involving a Co–Co antibonding LUMO of a_2 symmetry.

The calculations also suggest a high electron density on the apical carbon, which is consistent with the stability of the carbonium ions. This result implies that the rather low NQR frequency found for the Cl in $ClCCo_3(CO)_9$ is not due to a strong π donation but to a reduction in the amount of σ density donated by the Cl. There is, however, a small positive overlap population for the C–Cl π bond. In comparison with theoretical results on H_3CCl and HC≡CCl, the Cl ligand in $(CO)_9Co_3CCl$ donates more π density than it does in HC≡CCl and less σ density than it does in H_3CCl.

Neither the carbyne or the alkyl resonance structures provide an adequate description of the bonding in these clusters, but the localized MO model shown in **7** and **8** contains all of the essential features of the full MO treatment. Of the two approaches used in the complete MO treatment, 3 $Co(CO)_3$ plus CR or Co_3C plus 9 CO and R, the former was simpler because the Co–CO bonds cause a larger perturbation on the system than the formation of the Co–Co bonds. This suggests that ligated metal clusters may resemble very small supported clusters more closely than they do large metal clusters.

Acknowledgment is made to the Robert A. Welch Foundation (Grant A-648) and the National Science Foundation (Grant CHE 79-20993) for support of this work.

Registry No. $HCCo_3(CO)_9$, 15664-75-2; $CH_3CCo_3(CO)_9$, 13682-04-7; $CH_3OCCo_3(CO)_9$, 41751-68-2; $ClCCo_3(CO)_9$, 13682-02-5; $BrCCo_3(CO)_9$, 19439-14-6; $ICCo_3(CO)_9$, 41749-34-2.

(25) Baker, A. D.; May, D. P.; Turner, D. W. *J. Chem. Soc. B* **1968**, 22.